[PS]Earth Stress and Seismic Hazard from the Size-Frequency Distribution of Seismic Events*

Sherilyn Williams-Stroud[1] and Graham Yielding[2]

Search and Discovery Article #70278 (2017)**
Posted June 26, 2017

*Adapted from poster presentation given at AAPG 2017 Annual Convention and Exhibition, Houston, Texas, April 2-5, 2017
**Datapages © 2017 Serial rights given by author. For all other rights contact author directly.

[1]Confractus, Inc., Pasadena, California, United States (swilliamsstroud@gmail.com)
[2]Badley Geoscience Ltd, Hundleby, United Kingdom

Abstract

The parameter b in the 1942 Gutenberg-Richter Law (related to the parameter m in the 1939 Ishimodo-Iida relation) is used to describe the power-law relationship between the magnitude and total number of earthquakes in any given region and time period of at least that magnitude. The value of b is generally equal to 1.0 in seismically active regions, and variations in that value have been attributed to various causes including different stress regimes, source mechanism type, depth, and strength and heterogeneity of the rock. Workers applying this analysis to microseismicity have used it to interpret processes related to hydraulic fracturing treatments and have also interpreted b-values as a "stress meter" in the reservoir. If the b-value can indeed provide information about the stress state of the earth without a-priori knowledge of the tectonic setting, it could prove valuable for prediction of earthquake hazards related to induced seismicity by enabling predictions of the potential size and frequency of seismic events. By examining the b-value distribution of earthquake populations within the context of their geological history and present day geological setting, the validity of using stress meter interpretation appears to break down. An analysis of data from 3 case studies, a naturally occurring earthquake, microseismic data from a reservoir stimulation, and induced seismicity data from wastewater injection is presented, showing the relationships of the b-values to the mode of rock failure that generate the seismicity and the utility of an alternative, geologically-based explanation for b-value distributions. This alternative explanation for the b-value distribution can be used to quantify the nature of fault and fracture distributions in the reservoir in addition to providing a possible upper magnitude for potentially damaging earthquakes.

Selected References

Dempsey, D., J. Suckale, and Y. Huang, 2016, Collective Properties of Injection Induced Earthquake Sequences: 2. Spatiotemporal Evolution And Magnitude Frequency Distributions: Journal of Geophysical Research: Solid Earth, v. 121/5, p. 3638-3665.

Eaton, D.W., J. Davidsen, P.K. Pedersen, and N. Boroumand, 2014, Breakdown of the Gutenberg- Richter Relation for Microearthquakes Induced by Hydraulic Fracturing: Influence of Stratabound Fractures: Geophysical Prospecting, v. 62/4, p. 806-818.

El-Isa, Z.H., and D.W. Eaton, 2014, Spatiotemporal Variations in the b-value of Earthquake Magnitude–Frequency Distributions: Classification and Causes: Tectonophysics, v. 615, p. 1-11.

Gutenberg, B., and C.F. Richter, 1942, Earthquake Magnitude, Intensity, Energy, and Acceleration: Bulletin of the Seismological Society of America, v. 32/3, p. 163-191.

Gerstenberger, M., S. Wiemer, and D. Giardini, 2001, A Systematic Test of the Hypothesis that the b value Varies with Depth in California: Geophysical Research Letters, v. 28/1, p.57-60.

Heidbach, O, M. Rajabi, K. Reiter, and M. Ziegler, 2016, World Stress Map 2016: GFZ Data Services. http://doi.org/10.5880/WSM.2016.002 Website accessed June 2017.

Schorlemmer, D., S. Wiemer, and M. Wyss, 2005, Variations in Earthquake-Size Distribution across Different Stress Regimes: Nature, v. 437/7058, p. 539-542.

Scholz, C.H., 1968, The Frequency-Magnitude Relation of Microfracturing in Rock and its Relation to Earthquakes: Bulletin of the Seismological Society of America, v. 58/1, p. 399-415.

Yielding, G., M. Ouyed, G.C.P. King, and D. Hatzfeld, 1989, Active Tectonics of the Algerian Atlas Mountains - Evidence from Aftershocks of the 1980 El Asnam Earthquake: Geophysical Journal International, v. 99/3, p. 761-788.

Earth Stress and Seismic Hazard from the Size-Frequency Distribution of Seismic Events

Sherilyn Williams-Stroud, Confractus Inc and Graham Yielding, Badley Geoscience

Abstract

The parameter *b* in the 1942 Gutenberg-Richter relation (similar to the parameter *m* in the 1939 Ishimoto-Iida relation) is used to describe the relationship between the magnitude and total number or earthquakes of at least that magnitude in a given earthquake population. The value of *b* is generally equal to 1.0 in seismically active regions, and deviations from that value have been attributed to various causes; different stress regimes, source mechanism type, depth, rock strength, and heterogeneity of the crust. Workers applying this analysis to microseismicity have used it to interpret processes related to hydraulic fracture stimulation, and have also interpreted *b*-values as a "stress meter" in the reservoir. If the *b*-value can indeed provide information about the stress state of the earth without a-priori knowledge of the tectonic setting, it could prove valuable for prediction of earthquake hazards related to induced seismicity by enabling predictions of the potential size and frequency of seismic events. By examining the *b*-value distribution of earthquake populations within the context of their geological history and present day geological setting, the validity of using a stress meter interpretation appears to break down. An analysis of data from 3 case studies - a naturally occurring earthquake, microseismic data from a reservoir stimulation, and induced seismicity data from wastewater injection is presented here. The relationships of the *b*-values to the mode of rock failure that generate the seismicity appear to have an influence on the b-value, illustrating the utility of an alternative, geologically-based explanation for different *b*-values. This alternative explanation for the b-value variation can be used to quantify the nature of fault and fracture distributions in the reservoir in addition to providing a possible upper magnitude for potentially damaging earthquakes.

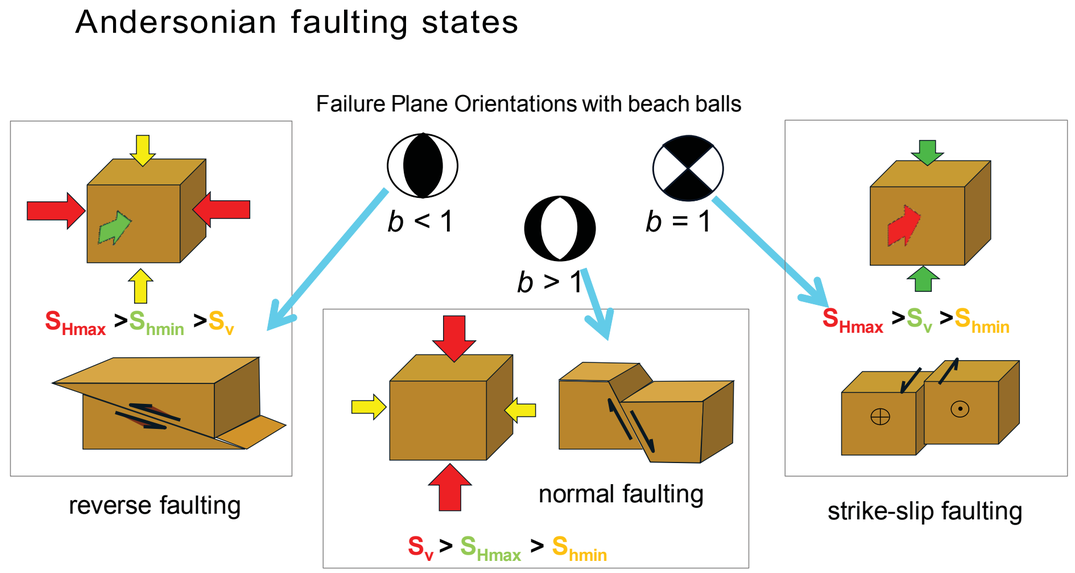

Figure courtesy of MicroSeismic Inc.

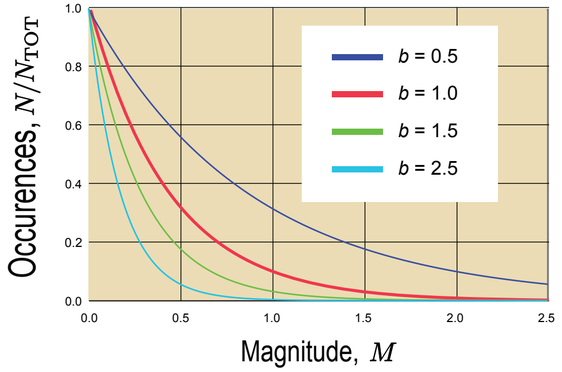

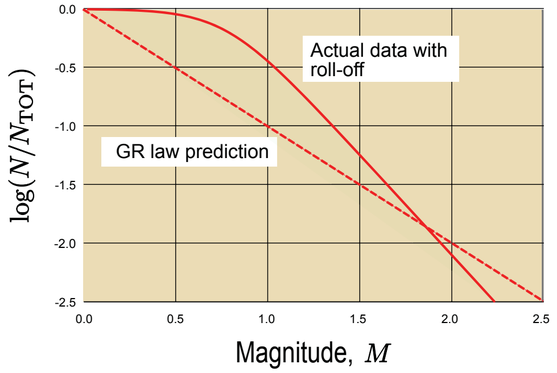

Image Source: https://en.wikipedia.org/wiki/Gutenberg-Richter_law

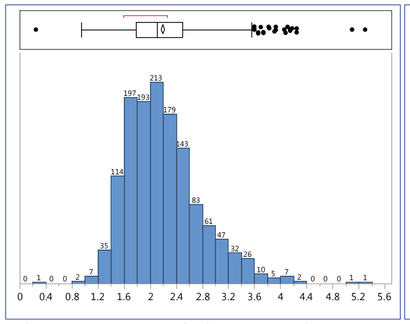

Size distribution of aftershocks from the El Asnam 1980 M 7.3 earthquake

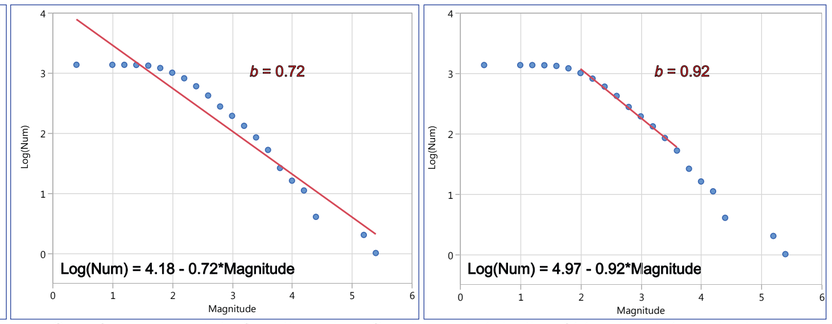

Size-frequency plot of earthquake aftershock distribution fit to all points including "rolloff" from under-sampled smaller events, and to only those magnitudes that are fully sampled (right).

What is the *b*-value?

It describes a type of self-similary found in the size distribution of earthquakes

- The distribution exhibits scale invariability
- It obeys power-law or fractal scaling
- Implies absence of a characteristic event size
- Self-similarity is also found in other geophysical and biological quantities... and in mapped faults.

If the b-value is greater than 1, it means that there is a relatively larger number of small earthquakes, if less than one, a relatively smaller number of small earthquakes. This is shown on the log-log plot as a steeper or shallower slope for the GR prediction.

Studies of *b*-value distributions by type of faulting (i.e., normal, strike-slip, or reverse) for earthquakes using their source mechanisms show:

$$b_{\text{Normal Faulting}} > 1 > b_{\text{Strike-Slip Faulting}} > b_{\text{Thrust Faulting}}$$

b-values from size-frequency analysis of three different natural earthquake populations. Events with M = 1.9 - 3.1 in Oklahoma have the largest *b*-value (= 1.03) which should indicate lower stress conditions. The smallest *b*-value is for an area of the Basin and Range Province in California; in both regions transtensional stress conditions exist, according to the World Stress Map. The intermediate *b*-value is for the an earthquake population in the California Transverse Ranges

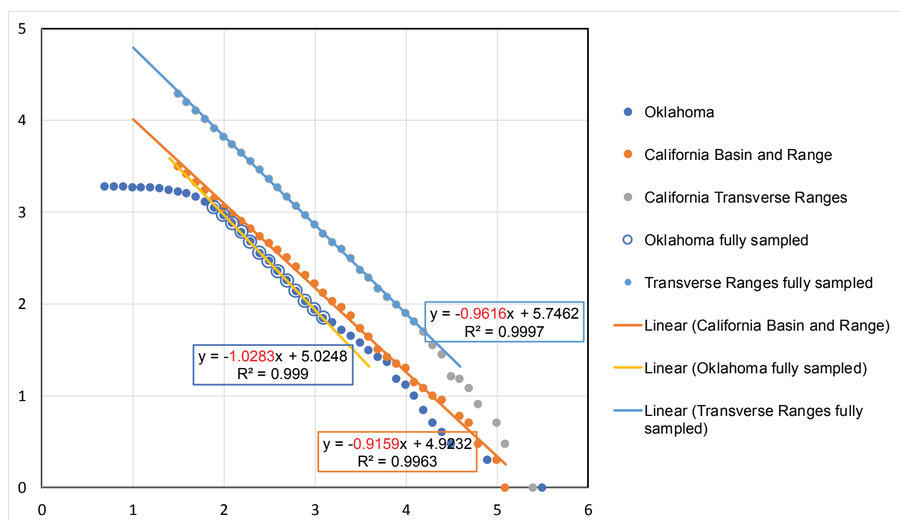

Earth Stress and Seismic Hazard from the Size-Frequency Distribution of Seismic Events

Sherilyn Williams-Stroud, Confractus Inc and Graham Yielding, Badley Geoscience

Stress and Faulting, Fault Size and Earthquakes, Fractures and Microseismicity

Faulting and rock failure are controlled by the rock strength and the stress tensor. The failure plane is related to the earthquake energy by

$M_0 = \mu AD$ *(Moment = Rigidity x FaultArea x SlipDistance*

The Moment represents the size of the rupture plane, and a higher b-value means a higher relative population of smaller rupture planes. Because of this relationship, the *b*-value could be primarily controlled by the failure plane size, rather than the mean stress.

The mean stress with depth (at a given depth) is higher for thrust faulting, which is higher than the mean stress in strike-slip faulting, which is higher than the mean stress for normal faulting.

The plots below show the Mohr stress circle for each of the end-member tectonic stress states and a corresponding stress versus depth plot. Any *new* faulting/earthquake fault plane solutions will be of the type represented by the source mechanism beachballs next to the Morhr stress circle plot.

In the case of existing faults, a range of orientations could be reactivated. In a structural inversion regime, for instance, if σ_1 and σ_3 are switched to orientations within the same plane, normal faults can reactivate as thrust faults.

The simplified conceptual diagrams (below) of normal and thrust fault geometry generalize the fault geometry and size relationships, illustrating how the *b*-value could be strongly influenced by existing faults and fractures in the rocks. This relationship holds for experimental rock deformation: low stress leads to brittle deformation with failure on more smaller failure planes, high stress leads to shear failure on a smaller number of larger failure planes.

$S_V = \sigma_1$

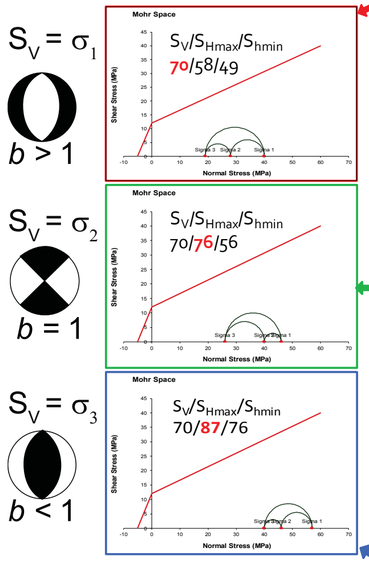

$S_V = \sigma_2$

$S_V = \sigma_3$

The red, green, or blue cross on the Stress v. Depth plots are S_V at 3000 meters depth.

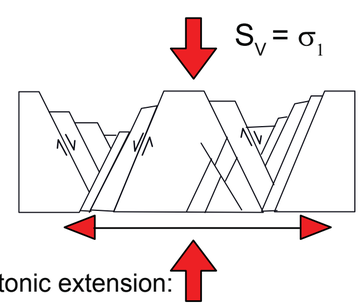

Tectonic extension:

Normal faulting -> more faults -> higher *b*-value

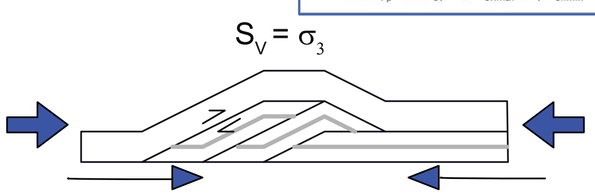

Tectonic compression:

Thrust faulting --> less faults --> lower *b*-value

An added influence on fault growth is mechanical stratigraphy. In normal faulting, fault growth can be arrested at bedding plane intersections, and in thrust faulting growth along the bedding planes could facilitate development of very large fault planes.

What might that look like in induced seismicity?

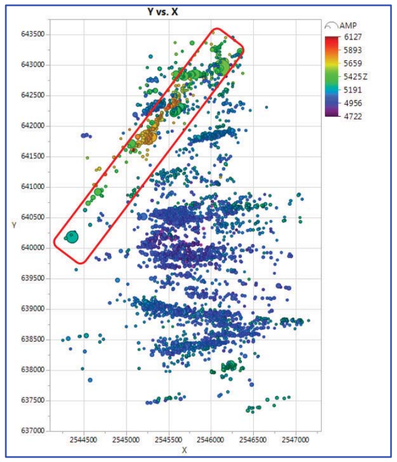

This mid-continent hydraulic fracture stimulation reactivated a fault in addition to creating and reactivating fractures during the treatment.

The fault events are larger than the rest of the microseismic population and have a lower *b*-value

Coloring the events by stage shows that the fault was encountered in stage 1, and continued to slip seismically for most of the 14 stages of treatment.

Coloring the events by rake as a proxy for the failure mechanism shows that the events in the fault are primarily strike-slip events. The *b* = 1 for the fault events, consistent with global *b*-value observations.

For the non-fault event population *b* = 1.8 and source mechanisms are dip-slip.

The depth of many of the fault events is mostly greater, so higher stress may be a factor.

Events colored by stage

Events Colored by rake*

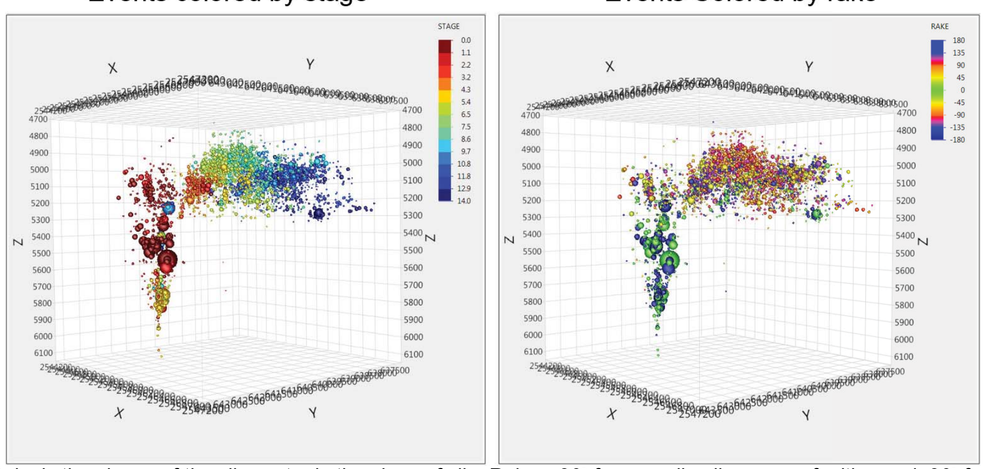

Rake is the plunge of the slip vector in the plane of slip. Rake = 90° for pure dip-slip reverse faulting and -90° for pure dip-slip normal faulting. Rake for pure strike-slip faulting = 0° for left-lateral and 180° for right lateral slip. In this plot green and blue colors denote either pure strike-slip or primarily strike-slip failure.

All Events

Fault Events

All non-Fault Events

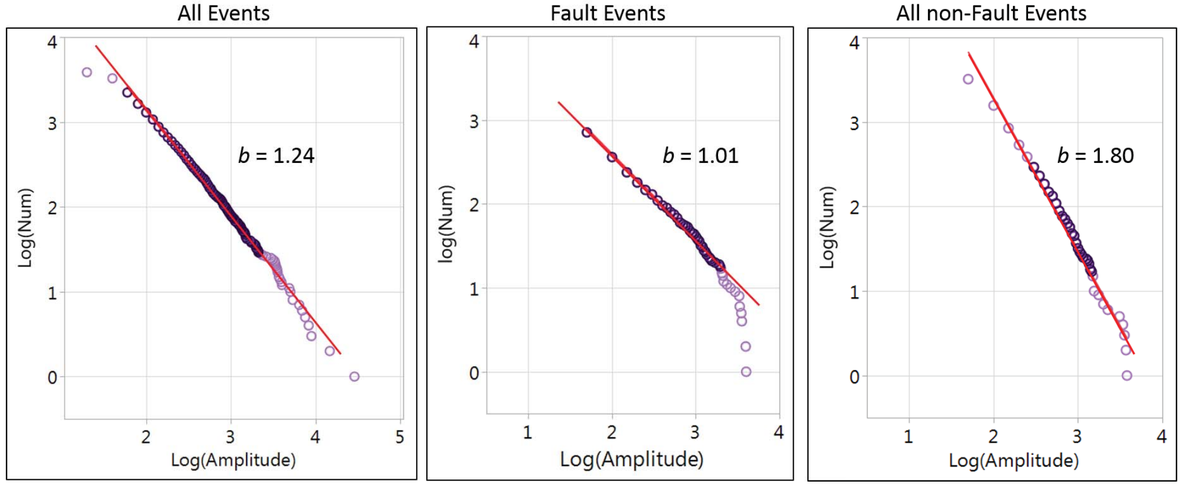

Earth Stress and Seismic Hazard from the Size-Frequency Distribution of Seismic Events

Sherilyn Williams-Stroud, Confractus Inc and Graham Yielding, Badley Geoscience

Natural seismicity *b*-values - 1980 El Asnam, Algeria, 7.3M Earthquake

The El Asnam (Algeria) earthquake of 1980 October is the largest earthquake to have occurred in North Africa since instrumental records began. It was caused by movement on a segmented reverse fault which is part of the fault zone that separates the Chelif alluvial plains from the coastal range of the Atlas Mountains. The coastal range is the actively deforming plate boundary between Africa and Eurasia.

The aftershock study was carried out using a 28-station portable network for 5 weeks after the mainshock. 4517 events were located, of which 1279 pass a set of quality criteria and were used to interpret detailed tectonics of the aftershock zone.

The seismicity in the southwestern half of the El Asnam fault zone had a relatively restricted band of seismicity running parallel to the main fault, occurring almost exclusively in the footwall, and indicating both antithetic reverse faulting and extension parallel to the fault zone.

The blind thrust broke the surface, creating a kilometers-long vertical scarp. The earthquake killed 5,000 people and caused severe damage.

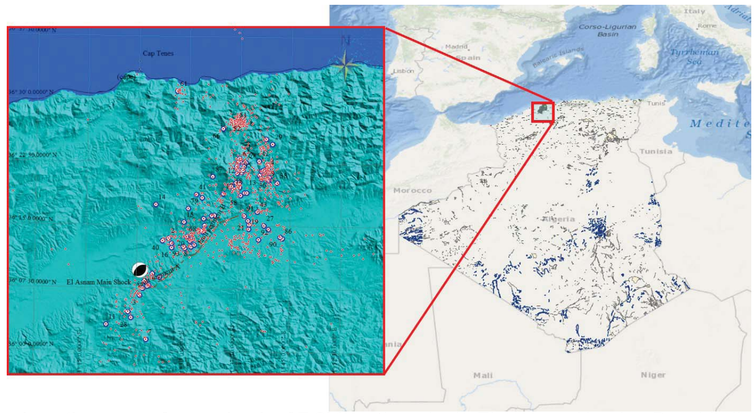

Location map of man shock of 7.3M earthquake in El Asnam, Algeria. Beachball shows location and source mechanism, or fault plane solution, of the reverse fault mainshock. Larger dots with blue outline have fault plane solutions. Smaller red dots are locations of >1200 well located aftershock events (w/o FPS).

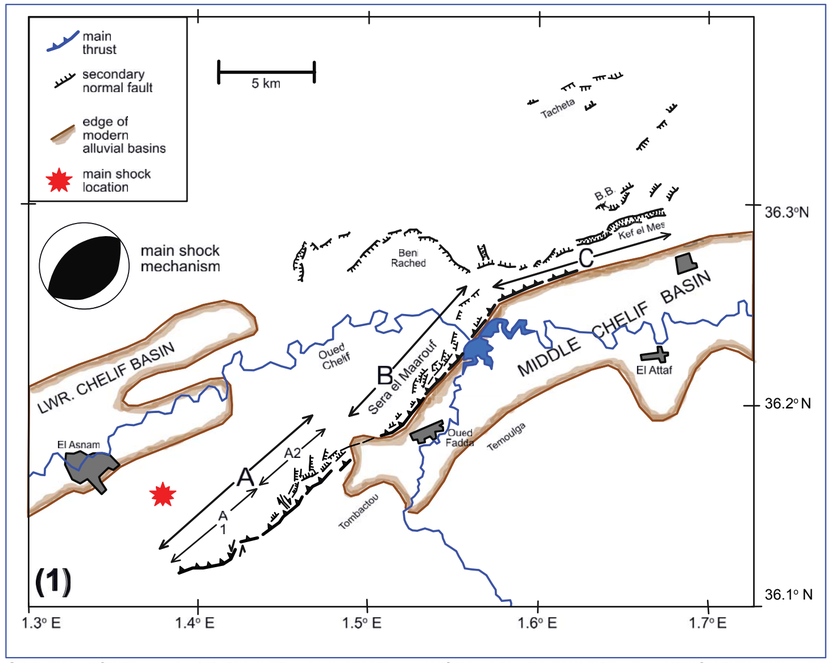

Structural features in El Asnam area showing surface breaks with three main fault segments.

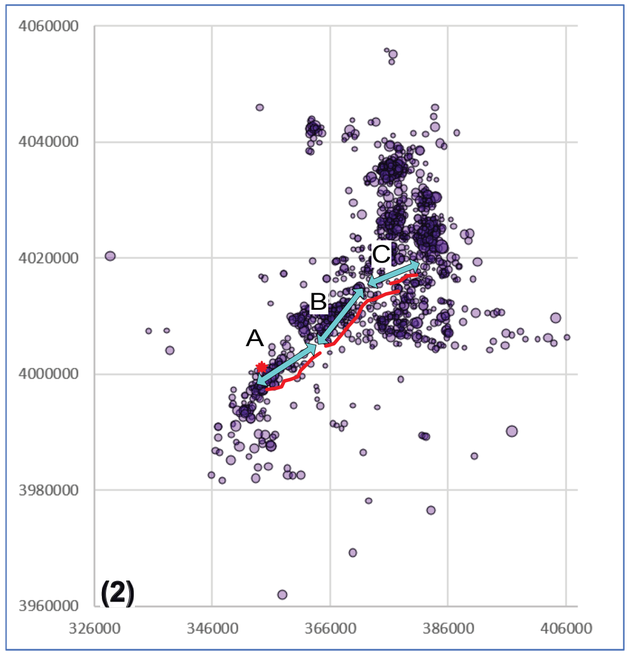

Map view of all aftershocks with fault segment locations superimposed. The red star is the location of the main shock.

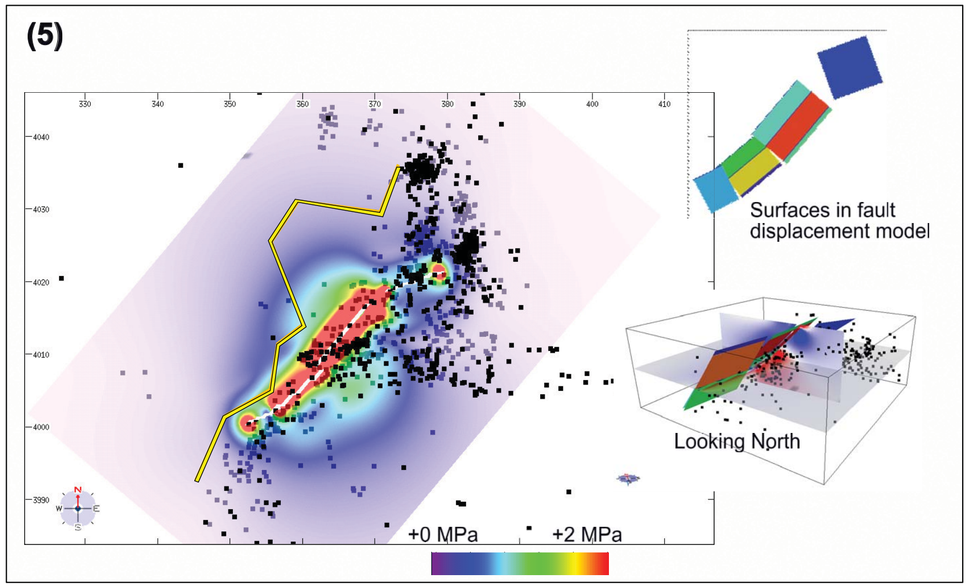

(5) Elastic dislocation model of stress on an observation plane at 6 km depth around the El Asnam fault at the time of rupture. The *b*-value distribution curve is superimposed, showing no relationship between stress magnitude and seismicity *b*-value.

The yellow line in figures 3, 4, and 5 denotes the *b*-values for different fault segments, ranging from ~ 0.75 to 1.35. The overall *b*-value for all located aftershocks was 1.03 ± 0.03 which is similar to the global average *b*-value associated with strike-slip failure. The mainshock rupture and the majority of the fault plane solutions (FPS) have a reverse faulting mechanism. Viewing the FPS events by depth, the high *b*-values that would be expected to be associated with lower mean stress, and therefore should be shallower, are associated with the the deepest large aftershocks as well as with shallow aftershocks (figure 4), and the full population of aftershocks in that sections appears equally distributed between very shallow and 10 km (figure 3). The differential stress calculated in the elastic dislocation model (Figure 5) shows no relationship to b-values.

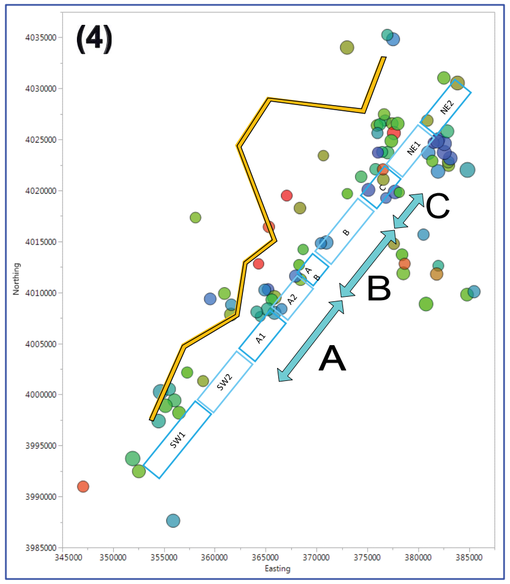

Map view of events with fault plane solutions, colored by depth.

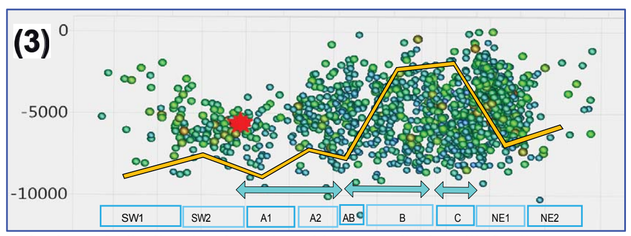

Depth view of all aftershocks colored by magnitude with fault segment locations indicated. The yellow line shows the *b*-values for events in each segment. Highest b-values occur near the bend between segment B and C.

Earth Stress and Seismic Hazard from the Size-Frequency Distribution of Seismic Events

Sherilyn Williams-Stroud, Confractus Inc and Graham Yielding, Badley Geoscience

Testing the hypothesis:

Pre-existing fault geometry influences seismicity *b*-value

In active faulting areas that have undergone only one tectonic deformation the surface fault geometry might be a reasonable indicator of the sub-surface fault distribution that could slip from earth stresses or that might be induced to slip from fluid production and injection.

To determine a "*b*" value for fault populations, the log of fault trace lengths were compiled and analyzed to compare to seismicity *b*-values from the same areas: Southern California and Oklahoma.

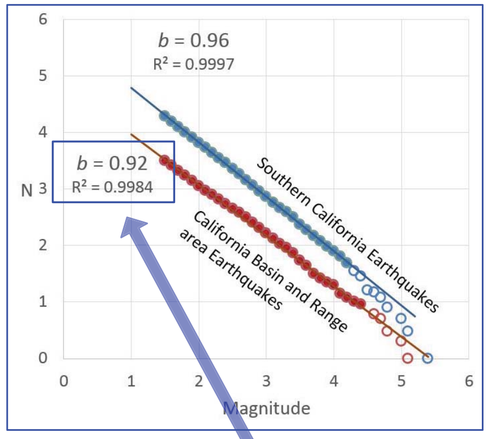

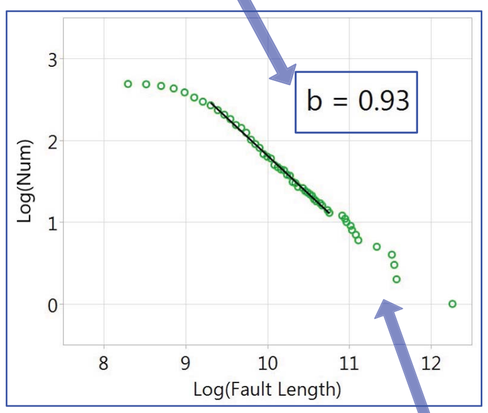

The seismicity *b*-value for the area inside the red box on the So. California map (below) is 0.92 for earthquakes recorded from 2007-2016

For the fault trace lengths in the same area, measured in ArcGIS software, *b* = 0.93.

Basin and Range tectonic stress is in an active transtensional regime. The strike-slip and normal faulting mechanisms are associated with *b* > 1. Here, earthquake *b* could be controlled by fault "*b*"

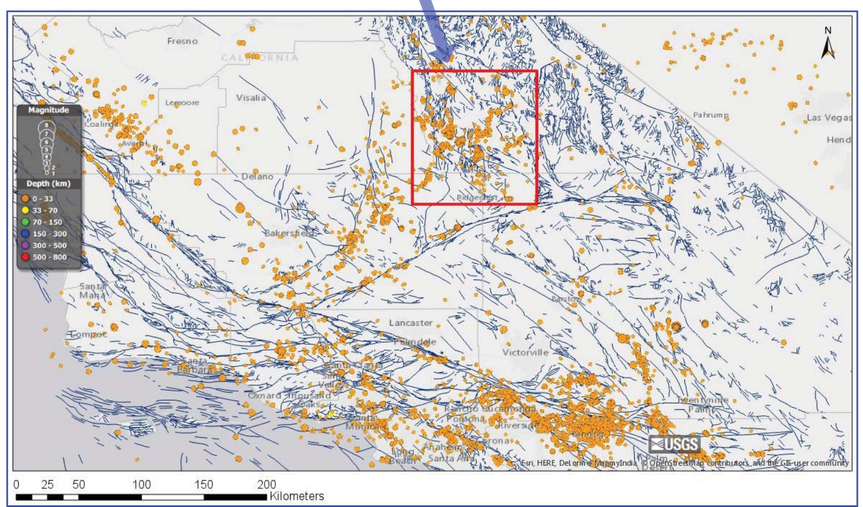

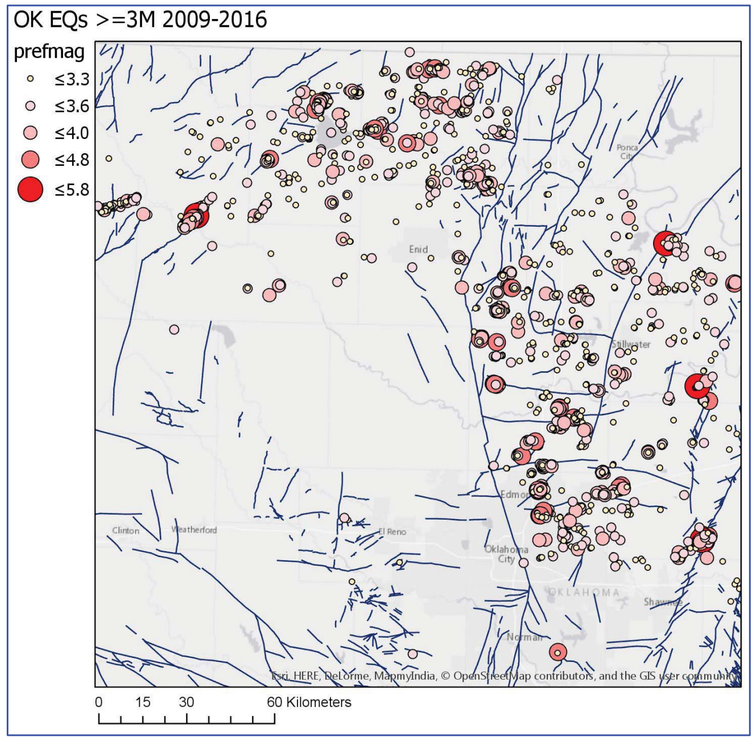

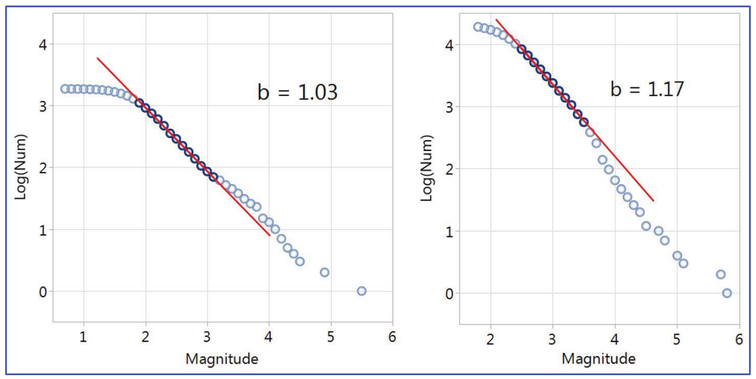

Oklahoma *b* values for seismicity prior to the sharp increase in induced seismicity (*b* = 1.03) and after (*b* = 1.17).

While M4 - M5 events were not unheard of historically, they were rare. The higher *b*-value for induced seismicity indicates more frequent smaller earthquakes.

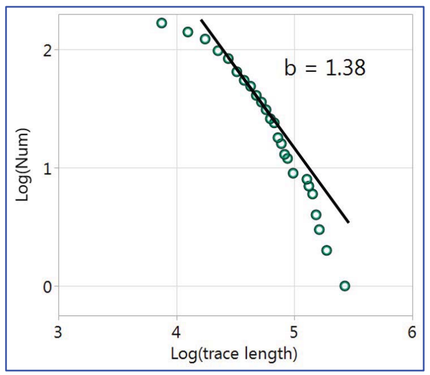

Because seismicity is higher now in general, more M>3 earthquakes, but (so far) the largest induced earthquakes are similar in magnitude to the largest historical earthquakes in Oklahoma.

Possible that the upper end of the curve is "pinned" by the fault sizes?

Fault "*b*" value (from map above) is higher than seismicity *b* value.

Conclusions

The *b*-value is a useful parameter to determine for a population of seismic events because it provides information about the nature of the associated rock failure. Characterization of the style of the discontinuities in the rock can be used to predict how frequently events will occur, and in particular, to estimate the likelihood and maximum size for a large and potentially damaging earthquake.

Taking in to consideration the previous structural deformation style shows that segregating *b*-values by time, or depth, or location can lead to ambiguous interpretations because it provides only a part of the story.

This work suggests that the relationships of the *b*-values to the mode of rock failure that generate the seismicity do have an influence on the b-value, illustrating the utility of an alternative, geologically-based explanation for different *b*-values. This alternative explanation for the b-value variation can be used to quantify the nature of fault and fracture distributions in the reservoir in addition to providing a possible upper magnitude for potentially damaging earthquakes.

References

Dempsey, David, Jenny Suckale, and Yihe Huang. "Collective properties of injection-induced earthquake sequences: 2. Spatiotemporal evolution and magnitude frequency distributions." *Journal of Geophysical Research: Solid Earth* 121, no. 5 (2016): 3638-3665.

Eaton, David W., Jörn Davidsen, Per Kent Pedersen, and Neda Boroumand. "Breakdown of the Gutenberg-Richter relation for microearthquakes induced by hydraulic fracturing: influence of stratabound fractures." *Geophysical Prospecting* 62, no. 4 (2014): 806-818

El-Isa, Z. H., and David W. Eaton. "Spatiotemporal variations in the b-value of earthquake magnitude–frequency distributions: Classification and causes." *Tectonophysics* 615 (2014): 1-11.

Gutenberg, Beno, and C_F Richter. "Earthquake magnitude, intensity, energy, and acceleration." *Bulletin of the Seismological Society of America* 32, no. 3 (1942): 163-191.

Gerstenberger, M., Wiemer, S. and Giardini, D., 2001. A systematic test of the hypothesis that the b value varies with depth in California. *Geophysical Research Letters*, *28*(1), pp.57-60.

Heidbach, Oliver; Rajabi, Mojtaba; Reiter, Karsten; Ziegler, Moritz (2016): World Stress Map 2016. GFZ Data Services. http://doi.org/10.5880/WSM.2016.002

Schorlemmer, Danijel, Stefan Wiemer, and Max Wyss. "Variations in earthquake-size distribution across different stress regimes." *Nature* 437, no. 7058 (2005): 539-542.

Scholz, C. H. "The frequency-magnitude relation of microfracturing in rock and its relation to earthquakes." *Bulletin of the Seismological Society of America* 58, no. 1 (1968): 399-415.

Yielding, G., M. Ouyed, G. C. P. King, and D. Hatzfeld. "Active tectonics of the Algerian Atlas mountains—evidence from aftershocks of the 1980 El Asnam earthquake." *Geophysical journal international* 99, no. 3 (1989): 761-788.